Impurity Limits in a Reactor Grade Fusion Device

T. Pütterich[1], E. Fable[1], R. Dux[1], R. Neu[1,2], M.G. O'Mullane[3], R. Wenninger[4]

[1]*Max-Planck-Institut für Plasmaphysik, D-85748 Garching, Germany*

[2]*Technische Universität München, 85748 Garching, Germany*

[3]*CCFE, Culham Science Centre, Abingdon, Oxfordshire OX14 3DB, United Kingdom*

[4]*EUROfusion Programme Management Unit, 85748 Garching, Germany*

Introduction and Production of Atomic Data Impurity limits for fusion devices are a topic of recent interest, because of several reasons. First, the implementation of first walls with high-Z elements (e.g. ITER-like wall in JET, full W-wall in ASDEX Upgrade) demonstrated the importance of impurity control. Second, it is well known that a substantial fraction of the heating power of a fusion reactor must be radiated via seeded impurities before the power flux enters the regions of the scrape-off layer. Third, a low-Z radiator for the divertor region is required in order to further reduce the power fluxes to the divertor. The atomic data of the radiators are usually derived from different types of calculations such that an investigation on the Z-scaling may suffer from artifacts. In order to avoid such systematic artifacts, atomic data for all considered elements (cf. Fig. 1) were produced by one set of codes from ADAS [1].

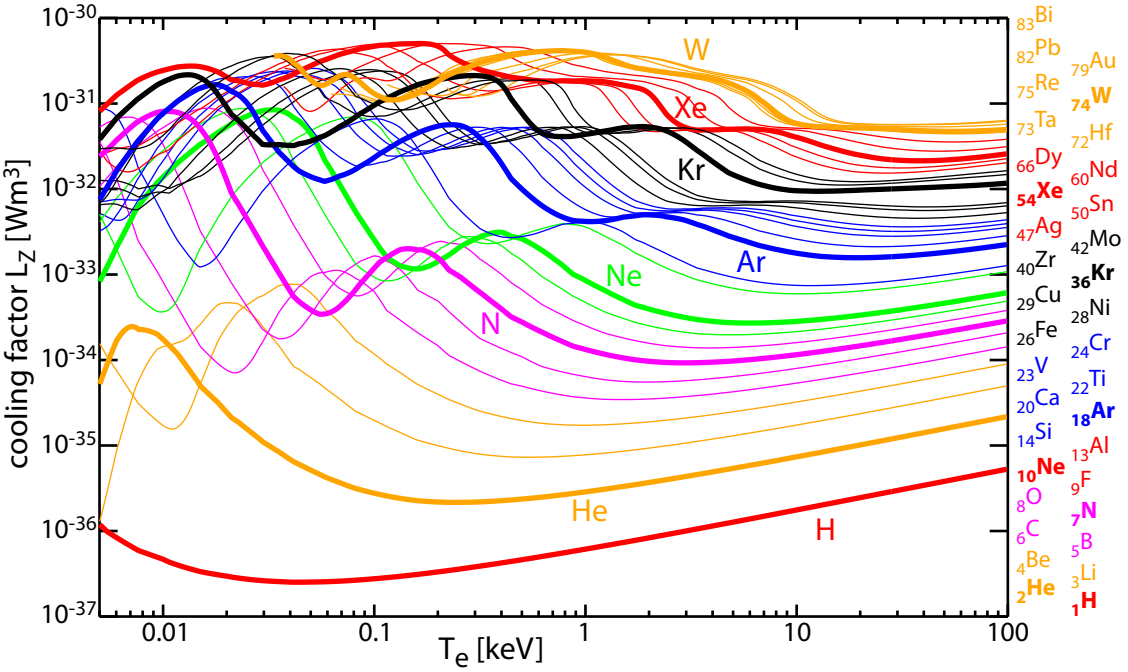

Fig. 1: *Calculated cooling factors for the considered elements from H to Bi.*

For all ion stages of the 35 elements under consideration, we used the Cowan code [2] via the infrastructure of ADAS to calculate the atomic/ionic structure and the electron impact collision cross sections (plane-wave Born). The spectra for each ion are then calculated using a collisional radiative model. For the cooling factor of the elements the configuration averaged scheme was used, as it is known to produce good radiation predictions [3]. For the determination of the recombination rates the 'type-A' implementation within the ADAS codes adas407/408 was used. For better results of these latter calculations all of the Cowan code calculations have been repeated using the intermediate coupling scheme. The latter also enables the prediction of detailed spectra for all elements. High-quality ionization rates were obtained via the configuration averaged distorted wave procedure of [4] using the ADAS implementation. As a result, we obtained a large set of radiation data for many elements including all

elements that may exists in a fusion plasma.

0D Reactor Model The investigated 0D model corresponds to case 4 in section 3 of [5]. The model basically balances the heating by alphas with the loss terms due to radiation and transport. For the radiation the cooling factors are used, while the power lost via transport is described by W/τ_E, where W is the stored thermal energy and τ_E is the energy confinement time. This balance provides the so-called burn condition and in the plane $nT\tau_E$ vs. T it is matched on the so-called burn curve. In order to treat the helium (He) ash self-consistently, it is assumed that the He confinement time τ_{He} is proportional to τ_E (cf. [5]). In the 0D approach the ratio $\rho^* = \tau_{He}/\tau_E$ must stay below 15.7 in order for a burn condition to exists, while in experiment values down to ≈ 4 have been observed [6]. In the present work the maximum impurity concentration is determined for a range of ρ^* and each impurity. Beyond that maximum impurity concentration no burn condition exists.

0.5D Reactor Model In order to take profile effects into account, the above model was extended via the parameters $\frac{T_{core}}{\langle T\rangle}$ and $\frac{n_{core}}{\langle n\rangle}$. $\frac{T_{core}}{\langle T\rangle}$ is the ratio of the core temperature and the volume averaged temperature, $\frac{n_{core}}{\langle n\rangle}$ is the ratio of the core density and the volume averaged density. The profiles themselves are assumed to be linear along the radial coordinate while a circular cross section of the plasma is assumed. This is thought to roughly approximate real plasmas, while plasma shape and profile shape dependencies are only mildly influencing the final result due to the parametrization using $\langle T\rangle$ and $\langle n\rangle$. This is confirmed by studies on the plasma elongation ϵ, which show that the influence of ϵ is negligible and thus, the effects of ϵ are not discussed further here. From the T- and n-profiles the α-heating profile and the radiated power profile are derived. Note that for $\frac{T_{core}}{\langle T\rangle} = \frac{n_{core}}{\langle n\rangle} = \epsilon = 1$ the results of the 0D model are reproduced.

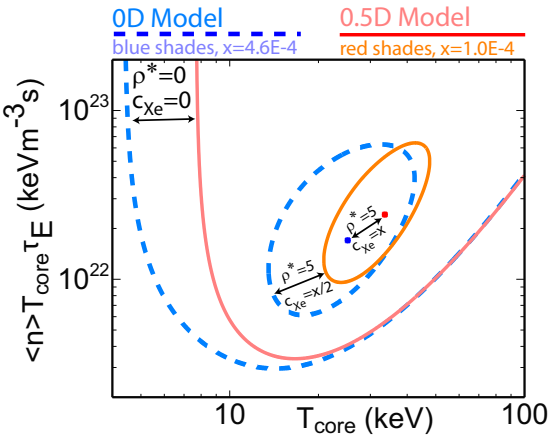

Fig. 2: *Burn curves for plasmas with no impurities and plasmas with He and Xe using the 0D-model (blue shades, dashed) and the 0.5D-model (red shades, solid).*

In Fig. 2, the burn curves are shown for the 0D model (dashed, blue shaded lines) and 0.5D model (solid, red shaded lines). The 0.5D model was evaluated for $\frac{T_{core}}{\langle T\rangle} = 2.0$, $\frac{n_{core}}{\langle n\rangle} = 1.3$ and $\epsilon = 1.8$, which corresponds approximately to the EU DEMO1 2015 design. For each of the two models, lines are presented that correspond to impurity-free plasmas ($\rho^* = 0$, $c_{Xe} = 0$), plasmas with He (assuming $\rho^* = 5$) plus xenon at the maximum concentration 'x' and half that value. Clearly, the consideration of profiles reduces the amount of tolerable xenon - for the considered cases from $4.6 \cdot 10^{-4}$ to $1.0 \cdot 10^{-4}$. In order to investigate this effect as a function of $\frac{T_{core}}{\langle T\rangle}$, $\frac{n_{core}}{\langle n\rangle}$ and ϵ the whole parameter space has been investigated with both models. Throughout the parameter space the consideration of profiles makes the burn condition harder to achieve and less impurities of any kind can be tolerated. This also leads to a reduction of the maximum ρ^* below of which a burn condition exists. The most unfavorable situation for a fixed T_{core} is achieved, when $\frac{T_{core}}{\langle T\rangle}$ is maximal (investigated up to $\frac{T_{core}}{\langle T\rangle} = 2.5$) and $\frac{n_{core}}{\langle n\rangle}$ is minimal (investigated down to $\frac{n_{core}}{\langle n\rangle} = 1$). A strong temperature peaking leads to a reduction of the plasma volume in which the optimal temperature is achieved and consequently causes a reduction of the impurity limit. Conversely, density peaking emphasizes the hot plasma region where the fusion power exceeds the radiated power and de-emphasizes the colder plasma volume where radiation is more important (if $\frac{n_{core}}{\langle n\rangle} > 1$).

The above 0.5D model is not directly applicable to a specific reactor design, because

within the 0.5D model the optimal $\langle n \rangle T_{core} \tau_E$ and T_{core} is chosen for each impurity independently. In reality, certain design parameters of a reactor fix the plasma parameters and the question is what the impurity limits are for that specific reactor design (SRD), e.g. for a specific core temperature. Thus, the above 0.5D model is extended further by finding the maximal impurity density at a fixed temperature (0.5D-SRD).

1D Reactor Model (ASTRA) The 0.5D-SRD model (here with $T_{core} = 25\,keV$) can be compared to a proper 1D model of a reactor design similar to that presented in [7]. The 1D ASTRA simulation takes into account the radiation and heating effects on a radial grid resembling the EU DEMO1 2015 design [8, 9]. This 1D ASTRA model allows to set a boundary condition on the radiative cooling, which is important to protect the divertor. In ASTRA the boundary condition on the power flux exiting the plasma is set to 1.2 times the power threshold for H-mode, i.e. 160 MW, such that a continuous operation in H-mode can be guaranteed. Note that this ignores the additional radiative cooling in the divertor, which is still important and may require a low-Z radiator such as nitrogen. It still makes sense to compare the 0D and 0.5D models with $Q = \frac{P_{fusion}}{P_{aux-heating}} = \infty$ to the 1D ASTRA model: First,the synchrotron radiation not considered in the 0D and 0.5D models is about equal to the 50 MW of auxiliary heating taking place for the EU DEMO1 2015 design. Second, meeting the condition of 160 MW power crossing the separatrix in the EU DEMO1 2015 design requires a major reduction of the power flux, which is approximately resembled by the 0D and 0.5D models where also a major fraction of the produced power is radiated or lost via dilution. In Fig. 3(a), results from all models are compared for N and Xe versus ρ^*. The 0D model allows for larger impurity concentrations than the 0.5D, the 0.5D-SRD and the 1D ASTRA model. The 0.5D-SRD model reproduces the 1D ASTRA results within a factor of ≈ 3 for $\rho^* < 6.5$. For $\rho^* \geq 6.5$ the 0.5D-SRD model results have not been evaluated, because the tolerable impurity content steeply drops, while in the 1D ASTRA simulation the impurities on top of He are more easily tolerated. However, in the 1D ASTRA model the fusion yield Q (numbers nearby data points) drops at larger ρ^*, such that large ρ^* must be avoided in a reactor for economical reasons. In fact, Q is alarmingly low in the 1D ASTRA simulation even for $\rho^* < 6.5$. For a conservative estimate of $\rho^* = 5$, the impurity limits are presented in Fig. 3(b) and Q ranges between 23 (using N) and 31 (using Xe). For $\rho^* = 5$, the 1D ASTRA model requires an impurity amount which is more than predicted by the 0.5D-SRD model and less than predicted by the 0D model. A major difference between the models is the resulting He-concentration, which is for the $Q = \infty$

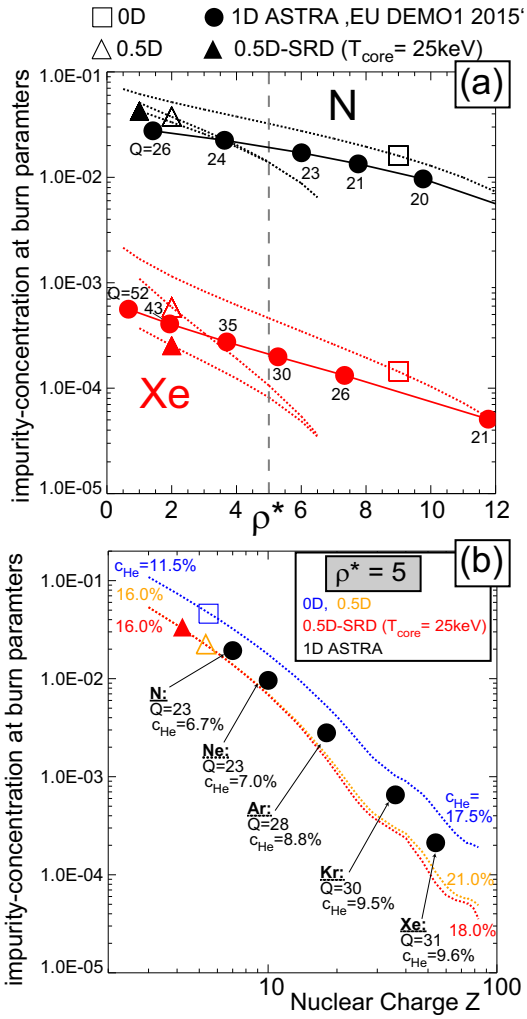

Fig. 3: *(a) Max. impurity concentration from all models for N, Ar, and Xe vs ρ^*. Numbers give Q for ASTRA runs. (b) Max. impurity concentration from all models vs. Z at $\rho^* = 5$. Q and He concentrations are also given.*

models approximately 2 times larger than in the 1D ASTRA model. Probably this is caused by the finite Q which allows for less He production at a certain τ_E.

In Fig. 4 a possible remedy for a too low Q is investigated. In Fig. 4(a), the effect of better confinement (red curves) and of an additional W-content of $c_W = 5 \cdot 10^{-5}$ (open symbols) on the tolerable/necessary Xe content is investigated with the 1D ASTRA model. Both the amount of the impurities and Q are increasing for an improved confinement factor (H-factor from ≈ 1.1 to ≈ 1.4). For an additional W content of $c_W = 5 \cdot 10^{-5}$ the required Xe content is decreased, while a negligible change of Q is observed. Q is almost unchanged because both Xe and W cause mostly radiation but negligible dilution. However, if N is considered as a plasma impurity instead of Xe (cf. Fig. 4(b)) the partial replacement of N by W leads to an increased Q due to the less severe dilution. Note that for all cases the density profile in the 1D ASTRA model is prescribed to match the EU DEMO1 2015 design, while a physics based model in ASTRA leads to a further reduction of Q. In conclusion, the low Q values found in the 1D ASTRA model w.r.t. to the predicted Q (i.e. 40 for the Xe case) by the DEMO1 design code requires further investigation. It hints to inconsistencies between the DEMO1 design code and the 1D ASTRA simulations. When comparing the 1D ASTRA model to the much simpler 0.5D models, the agreement for the tolerable impurity content are within a factor of 3 in the reactor relevant region of $\rho^* < 6.5$. The 0.5D model is largely independent of dimensions and geometry allowing for its application also in other devices such as stellarators or for a fast implementation in system codes. The 0D model gives always an upper limit to the impurity content.

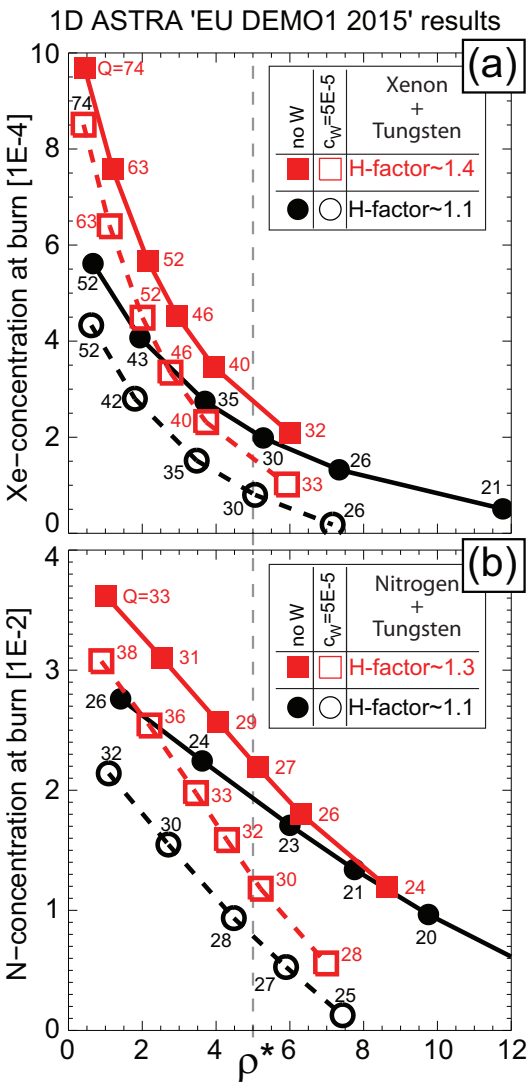

Fig. 4: *(a) Limit for Xe-concentrations vs. ρ^* for standard (black, circles) and increased H-factor (red, squares), for the case without W (filled symbols) and with a W-concentration of $5 \cdot 10^{-5}$ (open symbols). (b) Limit for N-concentrations vs. ρ^* for the same cases.*

References

[1] H. P. Summers, The ADAS User Manual, version 2.6 http://adas.phys.strath.ac.uk (2004).
[2] R. D. Cowan, *The Theory of Atomic Structure and Spectra* (University of California Press, 1981).
[3] T. Pütterich *et al.*, NF **50**, 025012 (9pp) (2010).
[4] S. D. Loch *et al.*, PRA **72**, 052716 (2005).
[5] D. Reiter *et al.* NF **30**, 2141 (1990).
[6] H.-S. Bosch *et al.*, PPCF **39**, 1771 (1997).
[7] R. Wenninger *et al.*, NF **54**, 114003 (2014).
[8] R. Wenninger *et al.*, *this conference, P4-110.*
[9] R. Kemp, private communication, 2015.

Acknowledgement This work has been carried out within the framework of the EUROfusion Consortium and has received funding from the Euratom research and training programme 2014-2018 under grant agreement No 633053. The views and opinions expressed herein do not necessarily reflect those of the European Commission